

Regression-Based Strategies to Reduce Refractive Error-Associated Glaucoma Diagnostic Bias When Using OCT and OCT Angiography

Keke Liu^{1,2}, Ou Tan¹, Qi Sheng You¹, Aiyin Chen¹, Jonathan C. H. Chan³, Bonnie N. K. Choy³, Kendrick C. Shih³, Jasper K. W. Wong³, Alex L. K. Ng³, Janice J. C. Cheung³, Michael Y. Ni⁴⁻⁶, Jimmy S. M. Lai³, Gabriel M. Leung⁴, Liang Liu¹, David Huang¹, and Ian Y. H. Wong^{3,7}

¹ Casey Eye Institute, Oregon Health & Science University, Portland, OR, USA

² John A. Burns School of Medicine, University of Hawai'i, Honolulu, HI, USA

³ Department of Ophthalmology, LKS Faculty of Medicine, The University of Hong Kong, The University of Hong Kong, Hong Kong, China

⁴ School of Public Health, LKS Faculty of Medicine, The University of Hong Kong, Hong Kong Special Administrative Region, Hong Kong, China

⁵ The State Key Laboratory of Brain and Cognitive Sciences, The University of Hong Kong, Hong Kong Special Administrative Region, China

⁶ Healthy High Density Cities Lab, HKUrbanLab, The University of Hong Kong, Hong Kong Special Administrative Region, China

⁷ Department of Ophthalmology, Hong Kong Sanatorium & Hospital, Hong Kong, China

Correspondence: Ian Y. H. Wong, Department of ophthalmology, The Hong Kong sanatorium and hospital, Happy Valley, Hong Kong, China. e-mail: ianyhwong@gmail.com

Received: August 23, 2021

Accepted: June 20, 2022

Published: September 16, 2022

Keywords: regressions; optical coherence tomography (OCT); glaucoma; magnification effect; false positives

Citation: Liu K, Tan O, You QS, Chen A, Chan JCH, Choy BNK, Shih KC, Wong JKW, Ng ALK, Cheung JJC, Ni MY, Lai JSM, Leung GM, Liu L, Huang D, Wong IYH. Regression-based strategies to reduce refractive error-associated glaucoma diagnostic bias when using OCT and OCT Angiography. *Transl Vis Sci Technol.* 2022;11(9):8, <https://doi.org/10.1167/tvst.11.9.8>

Purpose: The purpose of this study was to correct refractive error-associated bias in optical coherence tomography (OCT) and OCT angiography (OCTA) glaucoma diagnostic parameters.

Methods: OCT and OCTA imaging were obtained from participants in the Hong Kong FAMILY cohort. The Avanti/AngioVue OCT/OCTA system was used to measure the peripapillary nerve fiber layer thickness (NFLT), peripapillary nerve fiber layer plexus capillary density (NFLP-CD), macular ganglion cell complex thickness (GCCT), and macular superficial vascular complex vascular density (SVC-VD). Healthy eyes, including ones with axial ametropia, were enrolled for analysis.

Results: A total of 1346 eyes from 792 participants were divided into 4 subgroups: high myopia (<−6D), low myopia (−6D to −1D), emmetropia (−1D to 1D), and hyperopia (>1D). After accounting for age, sex, and signal strength, multivariable regression showed strong dependence in most models for NFLT, GCCT, and NFLP-CD on axial eye length (AL), spherical equivalent (SE) refraction, and apparent optic disc diameter (DD). Optical analysis indicated that AL-related transverse optical magnification variations predominated over anatomic variations and were responsible for these trends. Compared to the emmetropic group, the false positive rates were significantly (Chi-square test $P < 0.003$) elevated in both myopia groups for NFLT, NFLP-CD, and GCCT. Regression-based adjustment of these diagnostic parameters with AL or SE significantly (McNemar test $P < 0.03$) reduced the elevated false positive rates.

Conclusions: Myopic eyes are biased to have lower NFLT, GCCT, and NFLP-CD measurements. AL- and SE-based adjustments were effective in mitigating this bias.

Translational Relevance: Adoption of these adjustments into commercial OCT systems may reduce false positive rates related to refractive error.

Introduction

Optical coherence tomography (OCT) is one of the most used imaging modalities to diagnose glaucoma. OCT provides a reproducible quantitative assessment of structural damage in glaucoma, which often occurs before functional changes can be detected by perimetry.^{1,2} The peripapillary retinal nerve fiber layer thickness (NFLT) and the macular ganglion cell complex thickness (GCCT) have been used to detect and monitor glaucoma progression.^{3–5} More recently, OCT angiography (OCTA), an extension of OCT, has been used to measure the perfusion of different retinal layers.^{6–8} In the peripapillary region, glaucomatous damage can be best visualized in the nerve fiber layer plexus (NFLP) slab,^{9,10} whereas macular perfusion loss can be best observed in the superficial vascular complex (SVC) slab.¹¹ There is evidence that OCT angiography may improve the detection of glaucoma in the early stages.^{9,12,13}

In commercial OCT machines, individual ocular measurements are compared against a normative database to classify eyes as normal or abnormal. However, refractive error-associated biases present a challenge to accurate classification. For example, it is well known that the eye's axial length (AL) is inversely correlated to NFLT and GCCT due to optical magnification effects.^{14–20} Retinal anatomic changes associated with myopia and hyperopia further complicate the analysis. Ultimately, a regional or global reduction of NFLT due to myopia could cause a false positive diagnosis of glaucoma by an unwary clinician. This error is colloquially called the “red disease” because an abnormal classification is often printed in red in the output of the clinical OCT system.^{21,22} In OCTA, NFLP capillary density (CD) is negatively correlated with AL based on a nonlinear relationship.²³ Interestingly, many previous studies^{24–26} have not found a significant correlation between AL and macular SVC vessel density (VD).

With the rising prevalence of myopia projected to affect about 1 in 2 individuals by 2050, finding a solution to this diagnostic bias will be of increasing importance.²⁷ In the current study, we seek to correct this bias using clinically available measures of axial refractive error. These include the spherical equivalent (SE) manifest refraction (the standard measurement of myopia), AL, and apparent optic disc diameter (DD) measured on OCT. Although AL is not often measured in the eye clinic, it is essential in patients with cataract surgery or refractive surgery that dissociates the connection between the eye's refraction and optical magnification. We consider DD as a surrogate measure

of AL because it is strongly affected by the eye's optical magnification and is a convenient byproduct of OCT scanning of the disc region.

Methods

This cross-sectional study is based on a subgroup from the Hong Kong FAMILY Cohort population-based study, which includes a territory-wide random sample.²⁸ Of the 18 in Hong Kong, 4 districts (Tin Shui Wai, Sham Shui Po, Kwun Tong, and Tseung Kwan O) were selected. All participants aged 18 years and older in these districts were invited to participate. The Institutional Review Board of the University of Hong Kong approved the study which adhered to the Declaration of Helsinki. All participants provided written informed consent at enrollment. The recruitment process and cohort characteristics were previously reported.^{25,29} Comprehensive ophthalmic examination, systemic health questionnaire, and blood sampling were obtained from all participants. The AL was measured with an ocular biometer (AL-Scan, Nidek, Gamagori, Japan). The best-corrected visual acuity was measured by the best possible correction obtained by subjective refraction. DD was a direct output from the structural OCT scan.

Posterior segment imaging was obtained using a commercially available spectral-domain OCT device with OCTA function (Avanti with AngioVue OCTA, Optovue Inc., Fremont, CA, USA). The Avanti has a speed of 70,000 A-scans/second and an axial resolution of 5 μm full-width-half-maximum in tissue. Structural OCT scans of the optic nerve head region (ONH scan) were used to measure the NFLT at the standard 3.4-mm diameter circle, and structural OCT scans of the macula (GCC scan) shifted 1 mm temporal to the fovea were used to measure the GCCT in a 6 \times 6-mm area. The ONH scan also outputs the apparent optic disc area, which is converted to the apparent DD by assuming the disc is circular. A 6 \times 6-mm macular OCTA scan was used to measure the SVC-VD, and a 4.5 \times 4.5-mm OCTA scan of the optic disc region was used to measure peripapillary NFLP-CD. The OCTA scans were obtained with standard 304 \times 304 transverse sampling.

Only normal eyes were included in this study, and either one or two eyes were included per participant. Subjects with a history of glaucoma, abnormalities in frequency doubling technology (FDT) perimetry or fundus examination (disc, macula, or vessels), elevated intraocular pressure (>21 mm Hg), enlarged cup-to-disc ratio (>0.7), and pseudophakia were excluded. To

ensure quality, subjects with missing data or poor signal strength index (SSI), a measure of reflectance signal ranging from 0 to 100 based on OCT or OCTA scans (<50), were also excluded.

Both univariable and multivariable linear regression analyses were performed for each OCT parameter (NFLT, GCCT, NFLP-CD, and SVC-VD). The multivariable regression models always included age, sex, and SSI, whereas the measures of axial ametropia—AL, SE, and DD—were included in the model one at a time. The broken stick (or segmented) regression model related OCTA and OCT parameters to SE, AL, and DD, with the breakpoints set at emmetropia (SE = 0 diopters [D]). The slopes of the two segments in the broken stick model were considered significantly different if $P < 0.05$ for the interaction term between the axial ametropia variable and a variable that dichotomizes myopia versus hyperopia. To address the issue of within-participant clustering, a linear mixed model was applied to the multivariable regression analysis.

The coefficients from the regression models were then used to adjust OCT parameters for age, sex, SSI, and AL, SE, or DD. Therefore, OCT parameters following adjustment were labeled as AL-, SE-, or DD-adjusted. Pearson correlation coefficients were reported to compare the strengths of dependence among demographic or ocular characteristics and imaging parameters.

Eyes were divided into four groups based on SE: high myopia (<-6 D), low myopia (-6 to -1 D), emmetropia (-1 D to 1 D), and hyperopia (>1 D). The threshold for an “abnormal” classification was set at the fifth percentile of emmetropic eyes. Because all the subjects were normal, eyes with OCT and OCTA diagnostic parameters below the threshold were false positive abnormalities. The false positive rate was calculated by dividing the number of false positive eyes by the total number of eyes in each respective group. The false positive rate was used to measure the bias related to the refractive error. The chi-square test was used to determine the statistical significance of any difference in false positive rates between groups (e.g. emmetropia versus high myopia). The McNemar test was used to determine the statistical significance of any reduction in false positive rates derived from regression-based adjustments of diagnostic parameters.

The relative transverse optical magnification of OCT measurements made in an eye is estimated by the ratio of the eye’s AL to a reference AL.¹⁸ The reference is 23.82 mm, the AL of the optic model of the eye used by the Avanti OCT system to convert from the scan angles used to define scan pattern to

millimeter length on the retinal plane.³⁰ This magnification calculation was used to correct the magnification effect of AL variation on the measurements of DD and NFLT.

Statistical analysis was conducted in R using RStudio (RStudio for Mac, version 1.3; PBC, Boston, MA, USA). The linear mixed model multiple linear regression analysis was implemented using the lmerTest package.²¹ Figures were created using the ggplot2 package.^{31,32} GraphPad Prism version 9.0.2 for Mac (GraphPad Software, San Diego, CA, USA) was used to create figures highlighting the false positive rates. Last, statistical analysis (Pearson correlation coefficients, chi-square tests, and McNemar tests) was also performed in a random single-eye subset to ensure that any potential bias from clustering within participants does not significantly affect the results or conclusions.

Results

A total of 3936 eyes from 1968 participants were enrolled in the study. After excluding participants with a history of glaucoma or cataract and abnormalities on perimetry, tonometry, and fundus examinations, we included for analysis 1345 eyes from 792 participants with a mean \pm standard deviation of 46.6 ± 14.4 years (range = 18–78 years). All participants reported being of Asian ethnicity. Stratification by SE refraction showed myopia to be associated with younger age and higher intraocular pressure (Table 1), whereas hyperopes exhibit the opposite. As expected, myopes had significantly longer AL compared to emmetropes whereas the hyperopes had shorter AL. Consistent with the magnification effect, we observed reduced DD among the myopes and increased DD among the hyperopes. The magnification effect would also predict thinner NFLT and GCCT in the myopes, which was observed ($P < 0.004$ compared to emmetropes); however, thicker NFLT and GCCT were not observed among the hyperopes. In fact, NFLT among the hyperopes was slightly thinner compared to the emmetropes. A similar pattern was observed for the perfusion parameters NFLP-CD. Signal strength was highest in the emmetropes and decreased with any axial refractive error.

Because the effect of ametropia on OCT and OCTA parameters was only observed among the myopes and not the hyperopes (see Table 1), we used a broken stick model to separate the myopes and hyperopes in our regression analyses (Fig. 1). Linear regression showed that NFLT, NFLP-CD, and GCCT were significantly

Table 1. Demographic and Ocular Characteristics of Study Participants

Parameter	All	High Myopia (< -6 D)	Low Myopia (-6 D to -1 D)	Emmetropia (-1 D to 1 D)	Hyperopia (> 1 D)	<i>P</i> Value
Participants, <i>n</i>	792	66	337	285	104	
Eyes, <i>n</i>	1345	117	593	482	153	
Age, y	47.0 ± 14.7	40.3 ± 11.3	42.0 ± 14.0	50.3 ± 13.9	58.2 ± 11.8	<0.001
Sex, % male	42	44	44	42	38	<0.001
IOP, mm Hg	13.7 ± 2.7	14.0 ± 2.5	14.1 ± 2.8	13.3 ± 2.7	13.0 ± 2.6	<0.001
CCT, μm	548.9 ± 34.5	551.3 ± 27.8	553.3 ± 33.6	545.3 ± 37.5	540.9 ± 31.0	0.51
SE, D	-1.8 ± 2.9	-7.9 ± 1.7	-3.1 ± 1.4	0.1 ± 0.6	2.0 ± 1.3	<0.001
AL, mm	24.5 ± 1.4	26.7 ± 1.0	25.0 ± 0.9	23.7 ± 1.0	23.2 ± 1.1	<0.001
DD, mm	1.60 ± 0.17	1.50 ± 0.18	1.56 ± 0.16	1.65 ± 0.16	1.68 ± 0.16	<0.001
NFLT, μm	100.5 ± 9.2	95.2 ± 8.4	99.2 ± 9.0	102.9 ± 8.2	102.8 ± 9.5	<0.001
NFLT SSI	66.8 ± 8.0	64.6 ± 7.4	67.3 ± 7.6	66.8 ± 8.2	64.1 ± 8.5	<0.001
NFLP-CD, % area	54.2 ± 2.9	53.0 ± 3.0	54.0 ± 2.9	54.7 ± 2.7	54.0 ± 2.7	<0.001
NFLP-CD SSI	66.8 ± 7.7	63.1 ± 6.2	66.6 ± 7.3	68.1 ± 8.0	66.0 ± 8.2	<0.001
GCCT, μm	96.3 ± 6.8	94.6 ± 7.4	95.4 ± 6.3	97.4 ± 6.8	97.4 ± 7.5	<0.001
GCCT SSI	71.8 ± 7.1	68.3 ± 5.5	71.3 ± 6.8	73.3 ± 7.2	71.4 ± 7.8	<0.001
SVC-VD, % area	48.1 ± 3.3	47.4 ± 3.0	48.0 ± 3.1	48.4 ± 3.4	47.9 ± 3.3	0.12
SVC-VD SSI	66.5 ± 6.5	62.6 ± 5.5	66.3 ± 6.3	67.8 ± 6.6	65.6 ± 6.8	<0.001

The study participants were stratified by SE and group statistics are displayed as mean ± standard deviation. The difference among groups of continuous and categorical (e.g. sex) variables was tested by generalized linear mixed models to address within-participant clustering. Age was tested by analysis of variance. SSI is an integer score from 0 to 100 based on the reflectance signal. AL, axial length; CCT, central corneal thickness; CD, capillary density; DBP, diastolic blood pressure; DD, disc diameter; GCCT, ganglion cell complex thickness; IOP, intraocular pressure; NFLT, nerve fiber layer thickness; NFLP, nerve fiber layer plexus; SBP, systolic blood pressure; SE, spherical equivalent refraction; SSI, signal strength index; SVC, superficial vascular complex; VD, vessel density.

negatively correlated with AL and positively correlated with SE and DD among the myopes. Correlation was strongest for NFLT. No significant trends were found in most hyperopic segments except NFLT and GCCT were positively correlated with DD. The slopes of the hyperopic and myopic segments were significantly different from each other in the two NFL-associated SE plots ($P < 0.03$ for NFLT and $P < 0.02$ for NFLP-CD). Among the myopes, SVC-VD was significantly negatively correlated with AL; but the correlations with SE and DD were not significant. No significant trend was found among the hyperopes. For all these regression analyses (see Fig. 1), we compared the broken stick (segmented) models with a nonsegmented model and found the broken stick model to fit the data significantly better (ANOVA, $P < 0.001$).

Univariable linear regression (Table 2) showed that older age and male sex were significantly associated with lower NFLT, NFLP-CD, and SVC-VD, but not GCCT. Higher SSI was significantly correlated with greater OCT and OCTA parameters. The angiographic parameters (NFLP-CD and SVC-VD) were more dependent on SSI than age or sex.

Multivariable broken stick linear regression (Table 3) showed that older age was associated with significantly lower peripapillary NFLT, NFLP-CD, macular GCCT, but not lower SVC-VD. Male sex, in most models, was significantly correlated with reduced NFLT, NFLP-CD, and SVC-VD, but not GCCT. Higher SSI was significantly associated with higher OCT and OCTA parameters, but its effect (normalized slope) was much higher on the OCTA parameters compared to OCT parameters. In most models of myopic eyes, thinner NFLT and lower NFLP-CD were significantly associated with longer AL, lower SE, and smaller DD. In the macular region, GCCT had similar correlations with a smaller effect (normalized slope) compared to NFLT. Interestingly, reduced SVC-VD was weakly associated with lower SE and not significantly associated with AL or DD. The structural OCT parameters, NFLT and GCCT, have a stronger dependence on the axial myopia measures (AL, SE, and DD) than demographics (age and sex) and SSI. However, in NFLP-CD and SVC-VD, the reverse order was observed where SSI is the predominant effect, followed by sex, age, and axial myopia variables. Among the

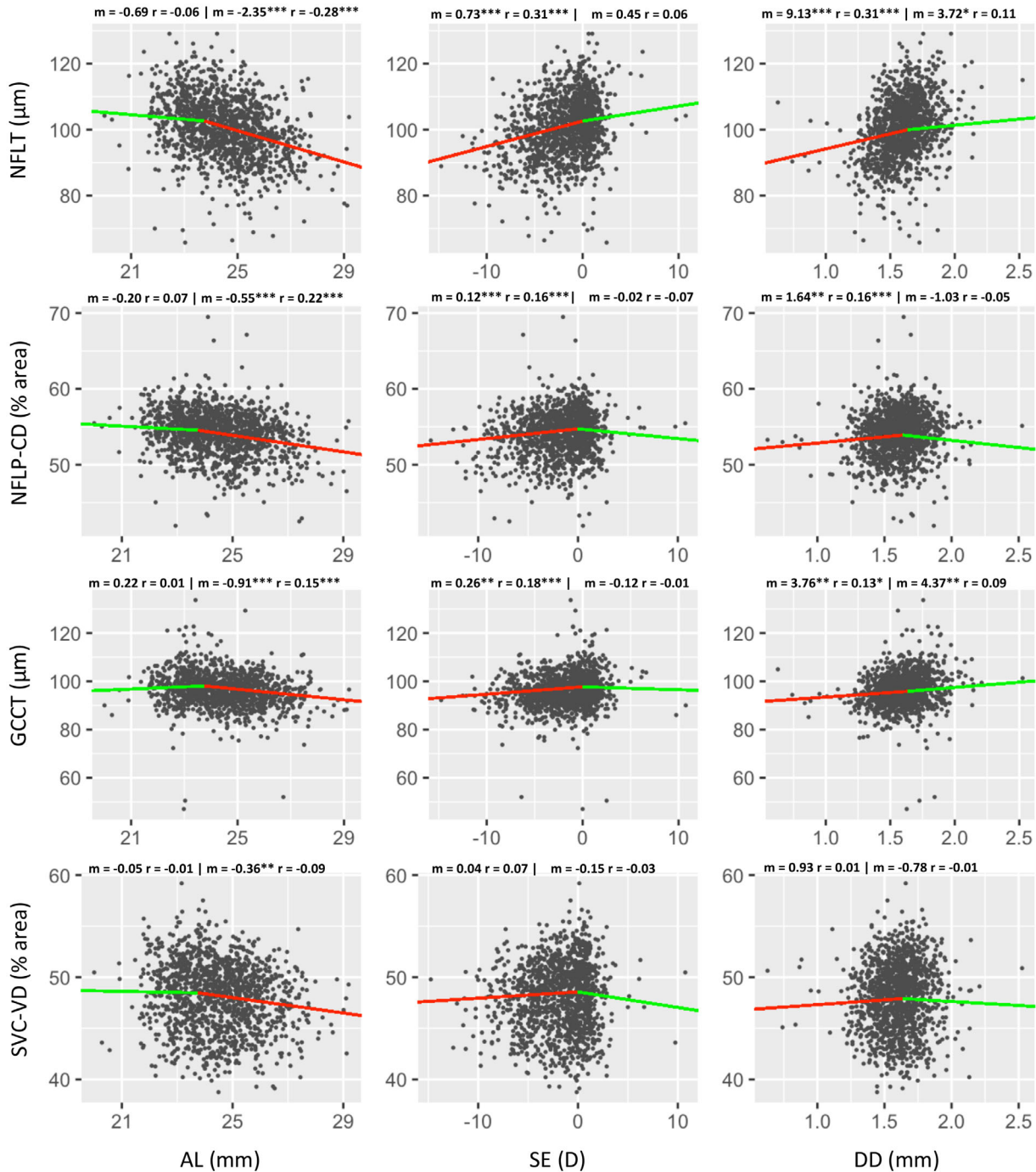


Figure 1. Plots of univariable broken stick regression fits between imaging-derived glaucoma diagnostic parameters and measures of axial ametropia. The breakpoints were set at AL = 23.76 mm, SE = 0.00 D, and DD = 1.64 mm. The *green segment* represents the hyperopic region, and the *red segment* represents the myopic region. The slope (m), statistical significance: ***($P < 0.001$), **($P < 0.01$), *($P < 0.05$), and Pearson correlation coefficient (r) are shown for each segment. AL, axial length; CD, capillary density; DD, disc diameter; GCCT, ganglion cell complex thickness; NFLT, nerve fiber layer thickness; NFLP, nerve fiber layer plexus; SE, spherical equivalence; SVC, superficial vascular complex; VD, vessel density.

axial myopia variables, AL and SE generally performed similarly well, but DD had the least effects as measured by normalized slope.

Compared to the emmetropic group, the false positive rates were significantly (chi-square tests $P <$

0.01) elevated in the high and low myopia group for NFLT, NFLP-CD, and GCCT (Fig. 2). SVC-VD was not significantly different from the emmetropia group, and this agrees with the regression models demonstrating a minimal correlation between SVC-VD and

Table 2. Effect of Demographics and Signal Strength on OCT and OCTA Parameters

Parameter	NFLT (μm)	NFLP-CD (% area)	GCCT (μm)	SVC-VD (% area)
Age (y)	-0.09*** (-0.12***)	-0.03*** (-0.16***)	-0.03 (-0.05*)	-0.03*** (-0.10***)
Sex (male: female)	-1.87** (-0.09***)	-1.08*** (-0.18***)	0.03 (0.02)	-0.92*** (-0.14***)
SSI	0.10*** (0.09***)	0.18*** (0.52***)	0.09*** (0.13***)	0.31*** (0.61***)

Univariable linear regression analyses were performed with NFLT, NFLP-CD, GCCT, and SVC-VD as dependent variables. Data are displayed as slope, statistical significance: ***($P < 0.001$), **($P < 0.01$), *($P < 0.05$), and Pearson r correlation coefficient (in parenthesis). Signal strength index (SSI) is an integer score from 0 to 100 based on the reflectance signal. CD, capillary density; GCCT, ganglion cell complex thickness; NFLT, nerve fiber layer thickness; NFLP, nerve fiber layer plexus; SSI, signal strength index; SVC, superficial vascular complex; VD, vessel density.

Table 3. Multivariable Linear Regression Analyses of Imaging Parameters

	NFLT (μm)	NFLP-CD (% Area)	GCCT (μm)	SVC-VD (% Area)
Model 1				
Age (y)	-0.14 (-0.23)***	-0.02 (-0.13)***	-0.05 (-0.10)**	0.01 (0.03)
Sex (% male)	-0.84 (-0.04)	-0.88 (-0.15)***	0.46 (0.04)	-0.97 (-0.15)***
SSI	0.08 (0.07)***	0.17 (0.46)***	0.06 (0.06)*	0.32 (0.63)***
AL (mm)	-2.57 (-0.33)***	-0.35 (-0.13)***	-0.97 (-0.20)***	0.11 (0.02)
Model 2				
Age (y)	-0.15 (-0.23)***	-0.03 (-0.12)***	-0.05 (-0.10)**	0.01 (0.03)
Sex (% male)	-1.67 (-0.10)**	-0.97 (-0.18)***	0.25 (0.00)	-0.93 (-0.14)***
SSI	0.09 (0.08)***	0.17 (0.47)***	0.06 (0.07)**	0.32 (0.64)***
SE (D)	0.88 (0.33)***	0.12 (0.14)***	0.29 (0.16)***	-0.08 (-0.08)*
Model 3				
Age (y)	-0.11 (-0.18)***	-0.02 (-0.11)***	-0.04 (-0.07)**	0.00 (0.03)
Sex (% male)	-1.41 (-0.10)*	-0.95 (-0.17)***	0.32 (0.01)	-0.96 (-0.14)***
SSI	0.08 (0.08)***	0.17 (0.48)***	0.06 (0.07)**	0.31 (0.63)**
DD (mm)	9.33 (0.15)***	0.82 (0.02)	3.61 (0.11)**	-0.17 (-0.01)

All broken stick regression models included age, sex, and SSI with the addition of AL (model 1), SE (model 2), or DD (model 3) separately in each model. The dependent variables are the column headings. Data are displayed as slope (slope normalized against standard deviation of both dependent and independent variable), and statistical significance: ***($P < 0.001$), **($P < 0.01$), *($P < 0.05$). The normalized slope is the change in standard deviation (SD) of the OCT parameter per 1 SD of the independent variable. Only the slopes for the myopic segments are shown; the slopes for the hyperopic segments were not statistically significant. SSI, signal strength index; AL, axial length; CD, capillary density; DD, disc diameter; GCCT, ganglion cell complex thickness; NFLT, nerve fiber layer thickness; NFLP, nerve fiber layer plexus; SE, spherical equivalence; SSI, signal strength index; SVC, superficial vascular complex; VD, vessel density.

measures of axial ametropia. No significant difference was found in false positive rates between the emmetropic and hyperopic groups, which agrees with the trends in diagnostic parameters among subgroups and supports the need for broken stick regression models to fit refractive error-associated biases better. Regression-based adjustment of diagnostic parameters with AL or SE significantly (McNemar test $P < 0.05$) reduced the false positive rates in the high and low myopia groups for NFLT, NFLP-CD, and GCCT (Fig. 3). Adjustment using DD did not significantly reduce the false positive rate for any diagnos-

tic parameter in any group. There was no significant difference between AL and SE adjustment, suggesting that they effectively remove diagnostic bias.

A case example was selected to demonstrate the utility of regression-based adjustment for OCT diagnostic parameters (Fig. 4). The right eye of a high myope with otherwise healthy eyes had OCT diagnostic parameters below the fifth percentile threshold of normal (false positive). After regression-based adjustment for AL, the parameters fell within the normal range (above the fifth percentile cutoff), and that eye is

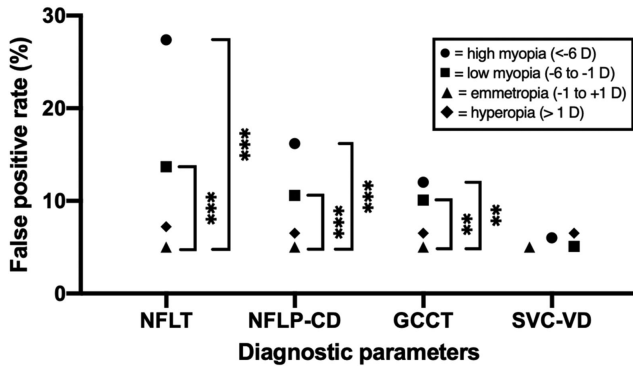


Figure 2. False positive rates of glaucoma diagnostic parameters stratified by refractive error based on shape. Adjustments in diagnostic parameters were made using multiple linear regression against age, sex, and signal strength index. Brackets between points indicate statistically significant differences from chi-square tests: ***($P < 0.001$), **($P < 0.01$). No statistical significance was found between hyperopia and emmetropia in NFLT, NFLP-CD, and GCCT. No statistical significance was found between emmetropia and all other subgroups in SVC-VD. CD, capillary density; GCCT, ganglion cell complex thickness; NFLT, nerve fiber layer thickness; NFLP, nerve fiber layer plexus; SVC, superficial vascular complex; VD, vessel density.

no longer considered a false positive. SE-based adjustment achieved similar results.

Using an AL-based model,¹⁸ we obtained magnification-corrected measurements for two quantities: DD and NFLT. Broken stick regressions were then implemented on both apparent and magnification-corrected measurements against AL (Fig. 5). The

magnification-corrected measurements reflect the actual anatomic variation, showing that longer eyes are associated with larger discs and thicker NFL. These associations were significantly stronger ($P < 0.04$) for hyperopic eyes. Without correction, the magnification effect predominates, resulting in the opposite trends where longer eyes are associated with smaller apparent DD and thinner apparent NFLT. These apparent associations were stronger for myopic eyes.

Discussion

In this large community-based study, we found that myopia correlates with increased false positive rates in OCT and OCTA parameters. The peripapillary parameters (NFLT and NFLP-CD) have stronger associations with AL than macular parameters (GCCT and SVC-VD). The diagnostic bias can be addressed by either AL- or SE-based adjustments using broken stick regression models.

This diagnostic bias in myopes has been documented in previous papers. In a study of 27 eyes, Rauscher et al. reported a higher prevalence of scans outside the normal limits based on the normative classification database in high myopes (50%; SE = < -5 D) compared to low myopes (15%).⁵ A study of 125 eyes by Leung et al. found a similar correlation where more eyes were classified as abnormal in the high myopia group than in the low-to-moderate myopia group.⁴ Furthermore, Chong and Lee cautioned against classifying eyes as normal or abnormal solely

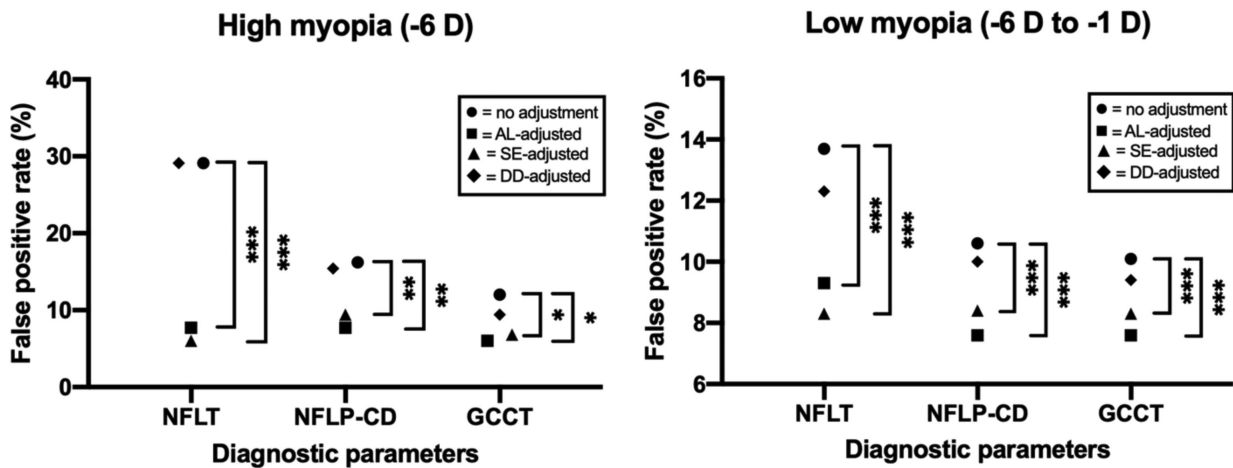
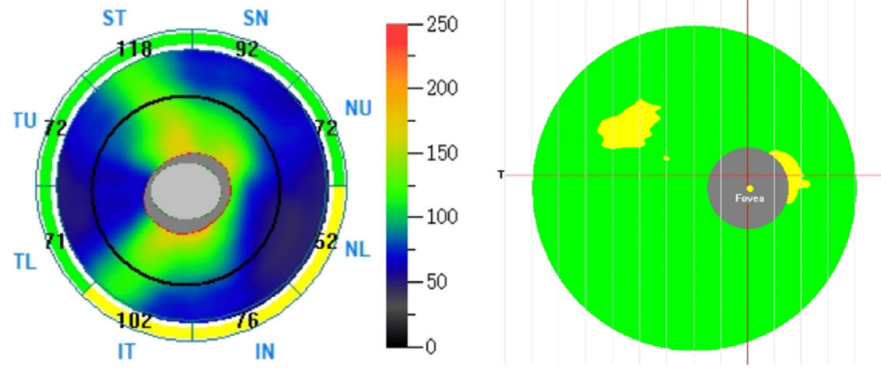


Figure 3. False positive rates of glaucoma diagnostic parameters stratified by adjustment type based on shape. Brackets between points indicate statistically significant differences from McNemar tests: ***($P < 0.001$), **($P < 0.01$), *($P < 0.05$). No statistical significance was found between AL- and SE-adjustment in NFLT, NFLP-CD, and GCCT. No statistical significance was found with or without DD-adjustment in NFLT, NFLP-CD, and GCCT. AL, axial length; CD, capillary density; DD, disc diameter; GCCT, ganglion cell complex thickness; NFLT, nerve fiber layer thickness; NFLP, nerve fiber layer plexus; SE, spherical equivalence.



	NFLT (μm)	NFLT Percentile	GCCT (μm)	GCCT Percentile
Original	82.06	2 nd	83.75	3 rd
AL-adjusted	92.03	14 th	88.56	10 th

Figure 4. An example case. The right eye of a 40-year-old man with an axial length of 28.56 mm is characterized as abnormal (below the fifth^h percentile threshold in emmetropic eyes) based on NFLT and GCCT measurements. (Left) Nerve fiber layer thickness map of the optic nerve head. (Right) Normative database reference map of the macular region. (Bottom) Diagnostic parameters and percentiles before and after axial length adjustment. GCCT, ganglion cell complex thickness; NFLT, nerve fiber layer thickness.

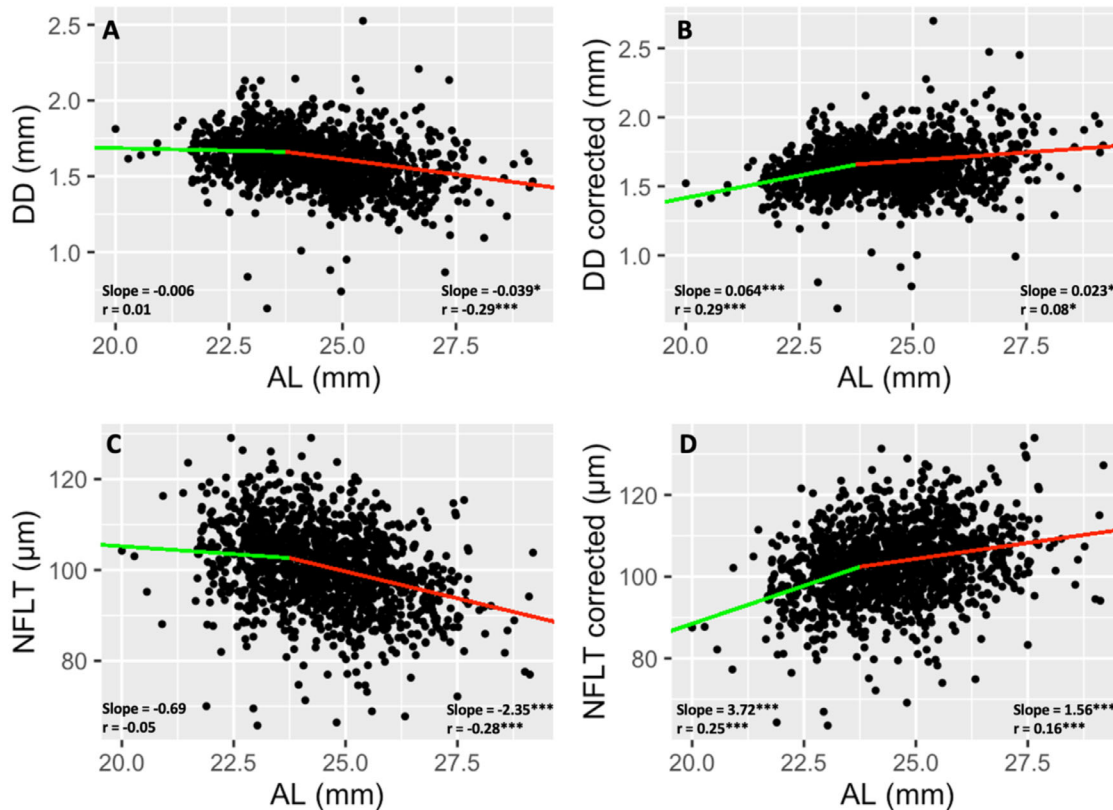


Figure 5. The impact of magnification correction on disc diameter and nerve fiber layer thickness. The apparent disc diameter (DD) (A) and the magnification-corrected DD (B) are plotted against axial length (AL). The apparent nerve fiber layer thickness (NFLT) (C) and the magnification-corrected NFLT (D) are plotted against axial length. The transverse optical magnification is calculated based on the axial length as described in the methods section. The broken stick model is used in linear regression with the breakpoint set at AL = 23.76 mm. The green segment represents the hyperopic region, and the red segment represents the myopic region. The slope, statistical significance: ***($P < 0.001$), **($P < 0.01$), *($P < 0.05$), and Pearson r correlation coefficient are shown for each segment.

on a normative database, especially when eyes do not match the characteristics of the database (e.g. high myopia).²¹

The optical magnification effect of imaging systems is one of the major contributing factors to the negative correlation between structural parameters and AL—leading to elevated false positive rates in myopic eyes. The magnification effect, a measurement artifact, explains that the actual transverse retinal dimension captured by the OCT scan pattern is larger in a myopic eye due to the greater distance subtended rays travel before reaching the retina.^{18,33} Magnification correction for NFLT is based on the knowledge that there are a fixed total number of nerve fibers in any individual eye. Assuming the nerve fiber and associated glial cross-sectional area are constant near the disc, a fixed total nerve fiber layer cross-sectional area. The measured overall average NFLT is the cross-sectional area divided by the circumference of the scan circle, which is inversely proportional to the magnification.

Previous reports have identified the effects of magnification and have attempted to correct this bias using the Littman or modified Bennet formulas.^{34–37} Certain studies using these formulas have also reported a positive correlation between NFLT and AL following correction.^{38–40} Our results, which also showed an increase in NFLT with longer AL after correction (see Fig. 5), support the notion that anatomically myopic eyes may have larger optic discs which are associated with a larger number of nerve fibers and, therefore, greater nerve fiber layer cross-sectional area.^{41–43} Hyperopic eyes exhibit an even stronger slope dependence, with the shorter eye having greatly reduced disc diameter and NFLT. The stronger dependence in hyperopic eyes could be explained by their relative lack of growth at a very early stage (3-9 months),^{44–46} thus resulting in fewer ganglion cells and nerve fibers. The weaker dependence in myopic eyes could be explained by the fact that axial elongation primarily occurs later during school age,⁴⁷ when the number of ganglion cells and nerve fibers is already fixed. The optical magnification effect may predominate in myopic eyes, resulting in the observed strong dependence of OCT and OCTA parameters on AL and axial refractive error. In contrast, anatomic variation and optical magnification effect may largely cancel in hyperopic eyes, explaining the weak dependence of OCT and OCTA parameters on AL and axial refractive error.

The decision to use broken stick regression models that separates the analyses of hyperopic and myopic eyes was based on the observation that hyperopic eyes did not exhibit significant associations between apparent (no magnification correction) NFLT, NFLP,

and GCCT with refractive error, in contrast with myopic eyes, which showed a strong association. This is in agreement with previous reports that studied NFLT.^{35,48} The significant difference in slopes between the myopic and hyperopic segments in the broken stick models of NFLT versus SE and NFLP-CD versus SE further justified the model. Furthermore, broken stick models exhibit a significantly better fit of the data ($P < 0.001$) compared to the unsegmented models. This advantage was found for all parameters.

Using the broken stick regression models, we found that both AL- and SE-based adjustments on NFLT, NFLP-CD, and GCCT can reduce the elevated false positive rates seen in myopic eyes. This is expected given that AL and SE are highly correlated, and both are reasonable measures of axial ametropia and associated magnification effect. Although we must remember that AL and SE can be dissociated surgically in patients after cataract and keratorefractive surgeries, these patients were not included in this study.

NFLP-CD, the angiographic counterpart to NFLT in the peripapillary region, demonstrated similar associations to measures of axial ametropia, albeit to a lesser extent. Compared to NFLT, which is analyzed over a circular scan, NFLP-CD is calculated from the summation of the overall percentage area representing microvasculature within the entire scan area—exhibiting a lower dependence on radius.^{18,49} Again, the magnification effect is likely the main contributing factor to the elevated false positive rates seen in the myopia subgroups compared to that of emmetropia. Consequently, OCT and OCTA studies conducted without magnification correction while hypothesizing that the nerve fiber thinning or vessel density decrease is due to excessive elongation of the eyeball in myopia should be interpreted with caution.^{5,26,50}

Compared to peripapillary parameters, macular parameters are less dependent on AL. We found that a 1-mm increase in AL resulted in an average decrease of 1.00% (0.97 μm) in GCCT compared to 2.50% (2.57 μm) in NFLT. Similarly, in a study of 74 participants without magnification correction, Takeyama et al. noted that GCCT decreased by 1.62 μm for each 1-mm increase in AL.¹⁶ This smaller AL dependence can be explained by the macular anatomy: the ganglion cell complex becomes thinner in the superior, inferior, and temporal directions as it traverses further from the center. But in the nasal direction, GCCT increases as one travels further from the foveal center and moves toward the optic disc, where the nerve fiber layer becomes very thick.⁵¹ These trends partially cancel each other. Empirically, the results show that GCCT still has small inverse dependence on AL, but the SVC-VD has no significant

dependence. Therefore, the macular SVC-VD may be a more reliable and unbiased measurement to assess highly myopic eyes without any AL or SE compensation. Even considering a potential magnification effect, a larger scan area in the macular region of a myopic eye will include vessels denser in the nasal region and sparser in the temporal—likely balancing out the overall VD. However, a recent study by Yang et al. found that SVC-VD decreased with increasing AL based on univariable analysis.⁵² We found a similar relationship in our univariable analysis, but this association disappeared when including age, sex, and signal strength index in a more robust multivariable regression analysis—agreeing with other studies.^{24–26} Taken all together, these observations suggest that the small effect of AL on SVC-VD may be primarily mediated by lower signal strengths in longer eyes.

We included DD in our study because it (apparent optic disc size as measured by OCT) is a surrogate measure for magnification obtained from OCT or OCTA scans of the disc without additional measurements or data entry. Smaller DD indicates either a lower transverse magnification (associated with axial myopia) or a physically smaller disc, which bias toward lower NFLT measurement in an otherwise normal eye. Thus, it is a reasonable basis for adjusting the normative range for NFLT and other OCT/OCTA diagnostic parameters. We found that decreased DD was associated with thinner NFLT and GCCT and lower NFLP-CD, in agreement with other studies.^{50,53–57} Nevertheless, DD-based adjustment of OCT/OCTA diagnostic parameters did not significantly improve the high false positive rate in myopic eyes. There are several possible explanations for this lack of efficacy. First, a decrease in DD due to a low magnification versus an actual smaller disc has different effects on NFLT and other OCT/OCTA parameters. So, DD may inappropriately conflate these two types of effects. Second, there is much random variation (scatter) in DD unrelated to AL variation. Third, disc tilt—often exaggerated in high myopes—may affect OCT measurements.^{58,59} Although the Optovue software measures DD in the Bruch's membrane opening plane, this may not altogether remove the effect of tilt on DD and NFLT measurements.⁶⁰ All of these factors may introduce noise and bias when DD is used as a basis of regression adjustment, making it less effective.

Besides AL and SE, other factors, such as age, SSI, and sex, should be adjusted in OCT/OCTA diagnostic parameters. Our regression models for NFLT, NFLP-CD, and GCCT agree with the majority of previous studies that have reported older age being associated with lower diagnostic parameters.^{53,61–67} Some studies failed to find this association, possibly due

to study populations with younger and narrower age ranges.^{4,5} We found that male sex was associated with lower NFLT, NFLP-CD, and SVC-VD but not for GCCT. Some reports agreed with our findings.^{66,67} Other studies failed to find a significant association between NFLT and sex, probably due to smaller sample sizes.^{5,53} Overall, our results support the use of age- and sex-adjusted (or stratified) normative data for the diagnostic classification of OCT and OCTA parameters. For OCTA parameters, SSI showed a more prominent effect than demographic variables and even AL or SE. A higher SSI is associated with a higher vessel and capillary density, an effect also reported in previous studies.^{66,68,69} The effect of SSI is due to the dependence of flow signal on OCT signal strength, and this bias can be removed by improving the measurement algorithm.⁷⁰ Ultimately, adjustment for SSI is crucial for NFLP-CD and SVC-VD values provided by current commercial OCTA systems.

There are several limitations of note in this study. The diagnostic parameters in this study are based on the mean of the entire scan, and sector analysis was not performed. Refractive error is known to affect the NFLT sector distribution,^{4,14,15} and we plan to analyze how this may affect the sector distribution of OCTA parameters in the future. Some statistical tests (Pearson correlation coefficients, chi-square tests, and McNemar tests) used in this study do not consider the potential bias from clustering within participants. To address this, these statistical methods were repeated using a random single-eye subset to ensure that the results and conclusions do not differ significantly from the current dataset including both eyes.

In conclusion, this population-based study uses regression-based strategies to adjust for confounding variables in diagnostic imaging parameters and demonstrate the utility of reducing false positive rates. Age, sex, SSI, and axial ametropia (as measured by either SE or AL) affect the measurements of NFLT, GCCT, NFLP-CD, and SVC-VD. These effects require compensation to avoid a frequent false-positive classification of abnormality. We anticipate a beneficial impact on clinical decision making with the adoption of these adjustments into commercial OCT systems.

Acknowledgments

The authors thank Dongseok Choi, PhD, at the Oregon Health & Science University for his statistical guidance. The Chloe Ho Safeguarding Vision Initiative was supported by The Jessie & George Ho Charitable Foundation. The establishment of the

original FAMILY Cohort was funded by the Hong Kong Jockey Club Charities Trust from 2007 to 2014. Funding for this project also came from National Institutes of Health (NIH) grants (R01 EY023285, R21 EY032146, and P30 EY010572), Research to Prevent Blindness/Allergan Foundation Medical Student Eye Research Fellowship, Champalimaud Foundation, and an unrestricted grant from Research to Prevent Blindness to Casey Eye Institute.

Disclosure: **K. Liu**, None; **O. Tan**, None; **Q.S. You**, None; **A. Chen**, None; **J.C.H. Chan**, None; **B.N.K. Choy**, None; **K.C. Shih**, None; **J.K.W. Wong**, None; **A.L.K. Ng**, None; **J.J.C. Cheung**, None; **M.Y. Ni**, None; **J.S.M. Lai**, None; **G.M. Leung**, None; **L. Liu**, None; **D. Huang**, None; **I.Y.H. Wong**, None

References

- Wollstein G, Schuman JS, Price LL, et al. Optical coherence tomography longitudinal evaluation of retinal nerve fiber layer thickness in glaucoma. *Arch Ophthalmol*. 2005;123(4):464–470.
- Ajtony C, Balla Z, Somoskeoy S, Kovacs B. Relationship between Visual Field Sensitivity and Retinal Nerve Fiber Layer Thickness as Measured by Optical Coherence Tomography. *Invest Ophthalmol Vis Sci*. 2007;48(1):258–263.
- Zhao Z, Jiang C. Effect of myopia on ganglion cell complex and peripapillary retinal nerve fibre layer measurements: a Fourier-domain optical coherence tomography study of young Chinese persons. *Clin Exp Ophthalmol*. 2013;41(6):561–566.
- Leung CK-S, Mohamed S, Leung KS, et al. Retinal nerve fiber layer measurements in myopia: An optical coherence tomography study. *Invest Ophthalmol Vis Sci*. 2006;47(12):5171–5176.
- Rauscher FM, Sekhon N, Feuer WJ, Budenz DL. Myopia affects retinal nerve fiber layer measurements as determined by optical coherence tomography. *J Glaucoma*. 2009;18(7):501–505.
- Jia Y, Tan O, Tokayer J, et al. Split-spectrum amplitude-decorrelation angiography with optical coherence tomography. *Opt Express*. 2012;20(4):4710–4725.
- Liu L, Jia Y, Takusagawa HL, et al. Optical Coherence Tomography Angiography of the Peripapillary Retina in Glaucoma. *JAMA Ophthalmol*. 2015;133(9):1045–1052.
- Hormel TT, Jia Y, Jian Y, et al. Plexus-specific retinal vascular anatomy and pathologies as seen by projection-resolved optical coherence tomographic angiography. *Prog Retin Eye Res*. Published online July 24, 2020:100878, <https://doi.org/10.1016/j.preteyeres.2020.100878>.
- Liu L, Edmunds B, Takusagawa H, et al. Projection-Resolved Optical Coherence Tomography Angiography of the Peripapillary Retina in Glaucoma. *Am J Ophthalmol*. 2019;207:99–109.
- Chen A, Liu L, Wang J, et al. Measuring Glaucomatous Focal Perfusion Loss in the Peripapillary Retina Using OCT Angiography. *Ophthalmology*. 2020;127(4):484–491.
- Takusagawa HL, Liu L, Ma KN, et al. Projection-Resolved Optical Coherence Tomography Angiography of Macular Retinal Circulation in Glaucoma. *Ophthalmology*. 2017;124(11):1589–1599.
- Yarmohammadi A, Zangwill LM, Manalastas PIC, et al. Peripapillary and Macular Vessel Density in Patients with Primary Open-Angle Glaucoma and Unilateral Visual Field Loss. *Ophthalmology*. 2018;125(4):578–587.
- Akil H, Huang AS, Francis BA, Sadda SR, Chopra V. Retinal vessel density from optical coherence tomography angiography to differentiate early glaucoma, pre-perimetric glaucoma and normal eyes. *PLoS One*. 2017;12(2):e0170476.
- Kim MJ, Lee EJ, Kim T-W. Peripapillary retinal nerve fibre layer thickness profile in subjects with myopia measured using the Stratus optical coherence tomography. *Br J Ophthalmol*. 2010;94(1):115–120.
- Wang G, Qiu KL, Lu XH, et al. The effect of myopia on retinal nerve fibre layer measurement: a comparative study of spectral-domain optical coherence tomography and scanning laser polarimetry. *Br J Ophthalmol*. 2011;95(2):255–260.
- Takeyama A, Kita Y, Kita R, Tomita G. Influence of axial length on ganglion cell complex (GCC) thickness and on GCC thickness to retinal thickness ratios in young adults. *Jpn J Ophthalmol*. 2014;58(1):86–93.
- Hirasawa K, Shoji N. Association between ganglion cell complex and axial length. *Jpn J Ophthalmol*. 2013;57(5):429–434.
- Huang D, Chopra V, Lu AT-H, Tan O, Francis B, Varma R. Does Optic Nerve Head Size Variation Affect Circumpapillary Retinal Nerve Fiber Layer Thickness Measurement by Optical Coherence Tomography? *Invest Ophthalmol Vis Sci*. 2012;53(8):4990–4997.
- Qu D, Lin Y, Jiang H, et al. Retinal nerve fiber layer (RNFL) integrity and its relations to retinal microvasculature and microcirculation in myopic eyes. *Eye and Vision*. 2018;5(1):25.

20. Seo S, Lee CE, Jeong JH, Park KH, Kim DM, Jeoung JW. Ganglion cell-inner plexiform layer and retinal nerve fiber layer thickness according to myopia and optic disc area: a quantitative and three-dimensional analysis. *BMC Ophthalmol.* 2017;17(1):22.
21. Chong GT, Lee RK. Glaucoma versus red disease: imaging and glaucoma diagnosis. *Curr Opin Ophthalmol.* 2012;23(2):79–88.
22. Silverman AL, Hammel N, Khachatryan N, et al. Diagnostic Accuracy of the Spectralis and Cirrus Reference Databases in Differentiating between Healthy and Early Glaucoma Eyes. *Ophthalmology.* 2016;123(2):408–414.
23. Jia Y, Simonett JM, Wang J, et al. Wide-Field OCT Angiography Investigation of the Relationship Between Radial Peripapillary Capillary Plexus Density and Nerve Fiber Layer Thickness. *Invest Ophthalmol Vis Sci.* 2017;58(12):5188–5194.
24. Wang Q, Chan S, Yang JY, et al. Vascular Density in Retina and Choriocapillaris as Measured by Optical Coherence Tomography Angiography. *Am J Ophthalmol.* 2016;168:95–109.
25. You QS, Chan JCH, Ng ALK, et al. Macular Vessel Density Measured With Optical Coherence Tomography Angiography and Its Associations in a Large Population-Based Study. *Invest Ophthalmol Vis Sci.* 2019;60(14):4830–4837.
26. Wang X, Kong X, Jiang C, Li M, Yu J, Sun X. Is the peripapillary retinal perfusion related to myopia in healthy eyes? A prospective comparative study. *BMJ Open.* 2016;6(3):e010791.
27. Holden BA, Fricke TR, Wilson DA, et al. Global Prevalence of Myopia and High Myopia and Temporal Trends from 2000 through 2050. *Ophthalmology.* 2016;123(5):1036–1042.
28. Leung GM, Ni MY, Wong PT, et al. Cohort Profile: FAMILY Cohort. *Int J Epidemiol.* 2017;46(2):e1.
29. You QS, Choy BKN, Chan JCH, et al. Prevalence and Causes of Visual Impairment and Blindness among Adult Chinese in Hong Kong - The Hong Kong Eye Study. *Ophthalmic Epidemiol.* 2020;27(5):354–363.
30. Sampson DM, Gong P, An D, et al. Axial Length Variation Impacts on Superficial Retinal Vessel Density and Foveal Avascular Zone Area Measurements Using Optical Coherence Tomography Angiography. *Invest Ophthalmol Vis Sci.* 2017;58(7):3065–3072.
31. Kuznetsova A, Brockhoff PB, Christensen RHB. lmerTest Package: Tests in Linear Mixed Effects Models. *Journal of Statistical Software.* 2017;82(1):1–26.
32. Wickham H. *Ggplot2: Elegant Graphics for Data Analysis.* New York, NY: Springer International Publishing; 2016.
33. Bayraktar S, Bayraktar Z, Yilmaz OF. Influence of scan radius correction for ocular magnification and relationship between scan radius with retinal nerve fiber layer thickness measured by optical coherence tomography. *J Glaucoma.* 2001;10(3):163–169.
34. Garway-Heath DF, Rudnicka AR, Lowe T, Foster PJ, Fitzke FW, Hitchings RA. Measurement of optic disc size: equivalence of methods to correct for ocular magnification. *Br J Ophthalmol.* 1998;82(6):643–649.
35. Öner V, Taş M, Türkcü FM, Alakuş MF, İşcan Y, Yazıcı AT. Evaluation of Peripapillary Retinal Nerve Fiber Layer Thickness of Myopic and Hyperopic Patients: A Controlled Study by Stratus Optical Coherence Tomography. *Current Eye Research.* 2013;38(1):102–107.
36. Savini G, Barboni P, Parisi V, Carbonelli M. The influence of axial length on retinal nerve fibre layer thickness and optic-disc size measurements by spectral-domain OCT. *Br J Ophthalmol.* 2012;96(1):57–61.
37. Wakitani Y, Sasoh M, Sugimoto M, Ito Y, Ido M, Uji Y. Macular thickness measurements in healthy subjects with different axial lengths using optical coherence tomography. *Retina.* 2003;23(2):177–182.
38. Hirasawa K, Shoji N, Yoshii Y, Haraguchi S. Determination of axial length requiring adjustment of measured circumpapillary retinal nerve fiber layer thickness for ocular magnification. *PLoS One.* 2014;9(9):e107553.
39. Kang SH, Hong SW, Im SK, Lee SH, Ahn MD. Effect of Myopia on the Thickness of the Retinal Nerve Fiber Layer Measured by Cirrus HD Optical Coherence Tomography. *Invest Ophthalmol Vis Sci.* 2010;51(8):4075–4083.
40. Nowroozizadeh S, Cirineo N, Amini N, et al. Influence of Correction of Ocular Magnification on Spectral-Domain OCT Retinal Nerve Fiber Layer Measurement Variability and Performance. *Invest Ophthalmol Vis Sci.* 2014;55(6):3439–3446.
41. Quigley HA, Brown AE, Morrison JD, Drance SM. The Size and Shape of the Optic Disc in Normal Human Eyes. *Archives of Ophthalmology.* 1990;108(1):51–57.
42. Jonas JB, Schmidt AM, Müller-Bergh JA, Schlötzer-Schrehardt UM, Naumann GO. Human optic nerve fiber count and optic disc size. *Invest Ophthalmol Vis Sci.* 1992;33(6):2012–2018.
43. Wang Y, Xu L, Zhang L, Yang H, Ma Y, Jonas JB. Optic disc size in a population based study in

- northern China: the Beijing Eye Study. *Br J Ophthalmol*. 2006;90(3):353–356.
44. Wildsoet CF. Active emmetropization—evidence for its existence and ramifications for clinical practice. *Ophthalmic Physiol Opt*. 1997;17(4):279–290.
 45. Smith EL, Hung LF. The role of optical defocus in regulating refractive development in infant monkeys. *Vision Res*. 1999;39(8):1415–1435.
 46. Mutti DO, Mitchell GL, Jones LA, et al. Axial Growth and Changes in Lenticular and Corneal Power during Emmetropization in Infants. *Invest Ophthalmol Vis Sci*. 2005;46(9):3074–3080.
 47. Iribarren R. Crystalline lens and refractive development. *Prog Retin Eye Res*. 2015;47:86–106.
 48. Lee JWY, Yau GSK, Woo TTY, Yick DWF, Tam VTY, Lai JSM. Retinal Nerve Fiber Layer Thickness in Myopic, Emmetropic, and Hyperopic Children. *Medicine (Baltimore)*. 2015;94(12):e699.
 49. Jia Y, Wei E, Wang X, et al. Optical Coherence Tomography Angiography of Optic Disc Perfusion in Glaucoma. *Ophthalmology*. 2014;121(7):1322–1332.
 50. Savini G, Zanini M, Carelli V, Sadun AA, Ross-Cisneros FN, Barboni P. Correlation between retinal nerve fibre layer thickness and optic nerve head size: an optical coherence tomography study. *Br J Ophthalmol*. 2005;89(4):489–492.
 51. Tan O, Li G, Lu AT-H, Varma R, Huang D. Mapping of Macular Substructures with Optical Coherence Tomography for Glaucoma Diagnosis. *Ophthalmology*. 2008;115(6):949–956.
 52. Yang D, Cao D, Zhang L, et al. Macular and peripapillary vessel density in myopic eyes of young Chinese adults. *Clin Exp Optom*. 2020;103(6):830–837.
 53. Budenz DL, Anderson DR, Varma R, et al. Determinants of Normal Retinal Nerve Fiber Layer Thickness Measured by Stratus OCT. *Ophthalmology*. 2007;114(6):1046–1052.
 54. Bendschneider D, Tornow RP, Horn FK, et al. Retinal Nerve Fiber Layer Thickness in Normals Measured by Spectral Domain OCT. *J Glaucoma*. 2010;19(7):475–482.
 55. Yamashita T, Sakamoto T, Yoshihara N, et al. Correlations Between Retinal Nerve Fiber Layer Thickness and Axial Length, Peripapillary Retinal Tilt, Optic Disc Size, and Retinal Artery Position in Healthy Eyes. *J Glaucoma*. 2017;26(1):34–40.
 56. Cheung CY, Chen D, Wong TY, et al. Determinants of Quantitative Optic Nerve Measurements Using Spectral Domain Optical Coherence Tomography in a Population-Based Sample of Non-glaucomatous Subjects. *Invest Ophthalmol Vis Sci*. 2011;52(13):9629–9635.
 57. Knight OJ, Girkin CA, Budenz DL, Durbin MK, Feuer WJ. Effect of Race, Age, and Axial Length on Optic Nerve Head Parameters and Retinal Nerve Fiber Layer Thickness Measured by Cirrus HD-OCT. *Arch Ophthalmol*. 2012;130(3):312–318.
 58. Shin H-Y, Park H-YL, Park CK. The effect of myopic optic disc tilt on measurement of spectral-domain optical coherence tomography parameters. *Br J Ophthalmol*. 2015;99(1):69–74.
 59. Hwang YH, Yoo C, Kim YY. Myopic Optic Disc Tilt and the Characteristics of Peripapillary Retinal Nerve Fiber Layer Thickness Measured by Spectral-domain Optical Coherence Tomography. *J Glaucoma*. 2012;21(4):260–265.
 60. Iverson SM, Sehi M. The comparison of manual vs automated disc margin delineation using spectral-domain optical coherence tomography. *Eye (Lond)*. 2013;27(10):1180–1187.
 61. Wang M, Elze T, Li D, et al. Age, ocular magnification, and circumpapillary retinal nerve fiber layer thickness. *J Biomed Opt*. 2017;22(12), <https://www.ncbi.nlm.nih.gov/pmc/articles/PMC5996149/pdf/JBO-022-121718.pdf>.
 62. Balazsi AG, Rootman J, Drance SM, Schulzer M, Douglas GR. The Effect of Age on the Nerve Fiber Population of the Human Optic Nerve. *Am J Ophthalmol*. 1984;97(6):760–766.
 63. Johnson BM, Miao M, Sadun AA. Age-related decline of human optic nerve axon populations. *AGE*. 1987;10(1):5–9.
 64. Peng PH, Hsu SY, Wang WS, Ko ML. Age and axial length on peripapillary retinal nerve fiber layer thickness measured by optical coherence tomography in nonglaucomatous Taiwanese participants. Bhattacharya S, ed. *PLoS One*. 2017;12(6):e0179320.
 65. Gadde SGK, Anegondi N, Bhanushali D, et al. Quantification of Vessel Density in Retinal Optical Coherence Tomography Angiography Images Using Local Fractal Dimension. *Invest Ophthalmol Vis Sci*. 2016;57(1):246–252.
 66. Rao HL, Pradhan ZS, Weinreb RN, et al. Determinants of Peripapillary and Macular Vessel Densities Measured by Optical Coherence Tomography Angiography in Normal Eyes. *J Glaucoma*. 2017;26(5):491–497.
 67. Ooto S, Hangai M, Tomidokoro A, et al. Effects of Age, Sex, and Axial Length on the Three-Dimensional Profile of Normal Macular

- Layer Structures. *Invest Ophthalmol Vis Sci.* 2011;52(12):8769–8779.
68. Cheung CYL, Leung CKS, Lin D, Pang C-P, Lam DSC. Relationship between retinal nerve fiber layer measurement and signal strength in optical coherence tomography. *Ophthalmology.* 2008;115(8):1347–1351, 1351.e1-2.
69. Rao HL, Addepalli UK, Yadav RK, Senthil S, Choudhari NS, Garudadri CS. Effect of scan quality on diagnostic accuracy of spectral-domain optical coherence tomography in glaucoma. *Am J Ophthalmol.* 2014;157(3):719–727.e1.
70. Gao SS, Jia Y, Liu L, et al. Compensation for Reflectance Variation in Vessel Density Quantification by Optical Coherence Tomography Angiography. *Invest Ophthalmol Vis Sci.* 2016;57(10):4485–4492.